

Supporting Information

**Dinuclear vs. Mononuclear Complexes: Accelerated, Metal-dependent Ring-Opening Polymerization of Lactide**

Mickael Normand,<sup>a</sup> Thierry Roisnel,<sup>b</sup> Jean-François Carpentier,<sup>a\*</sup> and Evgeny Kirillov<sup>a\*</sup>

1. Synthetic procedures and analytical data

2. NMR spectra

**Figure S1.**  $^1\text{H}$  NMR spectrum (500 MHz,  $\text{C}_6\text{D}_6$ , 298 K) of  $[\{\text{ON}^{\text{pipeBn}}\}\text{H}]_2$  (**II**).

**Figure S2.**  $^{13}\text{C}\{\text{H}\}$  NMR spectrum (125 MHz,  $\text{C}_6\text{D}_6$ , 298 K) of  $[\{\text{ON}^{\text{pipeBn}}\}\text{H}]_2$  (**II**).

**Figure S3.**  $^1\text{H}$  NMR spectrum (500 MHz,  $\text{C}_6\text{D}_6$ , 298 K) of  $[\{\text{ON}^{\text{pipeBn}}\}\text{AlMe}_2]_2$  (**II-Al<sub>2</sub>**).

**Figure S4.**  $^{13}\text{C}\{\text{H}\}$  NMR spectrum (125 MHz,  $\text{C}_6\text{D}_6$ , 298 K) of  $[\{\text{ON}^{\text{pipeBn}}\}\text{AlMe}_2]_2$  (**II-Al<sub>2</sub>**).

**Figure S5.**  $^1\text{H}$  NMR spectrum (500 MHz,  $\text{C}_6\text{D}_6$ , 298 K) of  $[\{\text{ON}^{\text{pipeBn}}\}\text{In}(\text{CH}_2\text{SiMe}_3)_2]_2$  (**II-In<sub>2</sub>**).

**Figure S6.**  $^{13}\text{C}\{\text{H}\}$  NMR spectrum (125 MHz,  $\text{C}_6\text{D}_6$ , 298 K) of  $[\{\text{ON}^{\text{pipeBn}}\}\text{In}(\text{CH}_2\text{SiMe}_3)_2]_2$  (**II-In<sub>2</sub>**).

**Figure S7.**  $^1\text{H}$  NMR spectrum (400 MHz,  $\text{C}_6\text{D}_6$ , 298 K) of  $\{\text{ON}^{\text{pipeBn}}\}^{\text{Ph}}\text{H}$  (**I<sup>Ph</sup>**).

**Figure S8.**  $^{13}\text{C}\{\text{H}\}$  NMR spectrum (100 MHz,  $\text{C}_6\text{D}_6$ , 298 K) of  $\{\text{ON}^{\text{pipeBn}}\}^{\text{Ph}}\text{H}$  (**I<sup>Ph</sup>**).

**Figure S9.**  $^1\text{H}$  NMR spectrum (400 MHz,  $\text{C}_6\text{D}_6$ , 298 K) of  $\{\text{ON}^{\text{pipeBn}}\}^{\text{Ph}}\text{AlMe}_2$  (**I<sup>Ph-Al</sup>**).

**Figure S10.**  $^{13}\text{C}\{\text{H}\}$  NMR spectrum (100 MHz,  $\text{C}_6\text{D}_6$ , 298 K) of  $\{\text{ON}^{\text{pipeBn}}\}^{\text{Ph}}\text{AlMe}_2$  (**I<sup>Ph-Al</sup>**).

3. Crystallographic data

**Figure S11.** Molecular structure of the bimetallic complex **II-In<sub>2</sub>**.

**Table S1.** Summary of Crystal and Refinement Data for Complexes **II-Al<sub>2</sub>** and **II-In<sub>2</sub>**.

#### 4. Kinetic data

**Figure S12.** Plot of *rac*-LA conversion (%) vs. time (s) for the binary system **[Al]**/iPrOH at different temperatures.

**Figure S13.** Plot of *rac*-LA conversion (%) vs. time (s) for the binary system **II–Al<sub>2</sub>**/iPrOH at different temperatures.

**Figure S14.** Plot of *rac*-LA conversion (%) vs. time (s) at 110 °C, at different concentrations of catalyst/initiator, with the binary system **II–Al<sub>2</sub>**/iPrOH.

**Figure S15.** Plot of  $\ln(k_{\text{app}})$  vs.  $\ln([\text{Al}])$  for ROP of *rac*-LA by the binary system **II–Al<sub>2</sub>**/iPrOH at 110 °C.

**Figure S16.** Plot of  $\ln(k_{\text{app}}/T)$  vs.  $1/T$  for ROP of *rac*-LA by the binary systems **I<sup>SiPh<sub>3</sub></sup>**–Al and **II–Al<sub>2</sub>**/iPrOH,  $[\text{rac-LA}]_0 = 2.0 \text{ M}$  in toluene.

**Figure S17.** Semi-logarithmic plots for ROP of *rac*-LA at 110 °C with  $[\text{rac-LA}]_0 = 2.0 \text{ M}$  in toluene for the binary systems **[In]**/iPrOH.

**Figure S18.** Plot of  $M_n$  vs. Conversion (%) for ROP with the binary systems **I<sup>SiPh<sub>3</sub></sup>**–Al and **II–Al<sub>2</sub>**/iPrOH.

#### 5. References and notes

## Experimental Part

**General Considerations.** All manipulations were performed under a purified argon atmosphere using standard Schlenk techniques or in a glove box. Solvents were distilled from Na/benzophenone (THF, Et<sub>2</sub>O) or Na/K alloy (toluene, hexane and pentane) under argon, degassed thoroughly and stored under argon prior to use. Deuterated solvents were stored over Na/K alloy (benzene-*d*<sub>6</sub>, toluene-*d*<sub>8</sub>, THF-*d*<sub>8</sub>; >99.5% D, Eurisotop) or CaH<sub>2</sub> (CD<sub>2</sub>Cl<sub>2</sub>) and vacuum-transferred just before use. CDCl<sub>3</sub> was dried over a mixture of 3 and 4 Å molecular sieves. 2,9-Dicarboxyaldehyde-1,8-bisphenol,<sup>1</sup> 2-hydroxybiphenyl-3-carbaldehyde<sup>2</sup> and precursors I<sup>SiPh<sub>3</sub></sup>-M (M = Al, In)<sup>3</sup> were prepared using literature procedures. *Racemic* lactide (*rac*-LA) was received from Acros. Purification of *rac*-LA required a three-step procedure involving first a recrystallization from a hot, concentrated *i*PrOH solution (80 °C), followed by two subsequent recrystallizations in hot toluene (100 °C). After purification, *rac*-LA was stored at a temperature of -30 °C in the glove-box. Other starting materials were purchased from Acros, Strem and Alfa and used as received.

**Instrumentation and Measurements.** NMR spectra of complexes were recorded on Bruker Avance DRX 400 and AM-500 spectrometers in Teflon-valved NMR tubes at 25 °C unless otherwise indicated. <sup>1</sup>H and <sup>13</sup>C NMR chemical shifts are reported in ppm vs. SiMe<sub>4</sub> and were determined by reference to the residual solvent peaks. Assignment of resonances for organometallic complexes was made from 2D <sup>1</sup>H-<sup>13</sup>C HMQC and HMBC NMR experiments.

Elemental analyses (C, H, N) were performed using a Flash EA1112 CHNS Thermo Electron apparatus and are the average of two independent determinations.

Size exclusion chromatography (SEC) analyses of PLAs were performed in THF (1.0 mL·min<sup>-1</sup>) at 20 °C using a Polymer Laboratories PL-GPC 50 plus apparatus equipped with two ResiPore 300 × 7.5 mm columns, and RI and Dual angle LS (PL-LS 45/90) detectors. The number-average molecular masses ( $M_n$ ) and polydispersity index ( $M_w/M_n$ ) of the polymers were

calculated with reference to a universal calibration *vs.* polystyrene standards. Reported experimental SEC molar mass values ( $M_{n,\text{SEC}}$ ) for PLA samples were corrected by a factor of 0.58,<sup>4</sup> as previously established. Unless otherwise stated, the SEC traces of the polymers all exhibited a unimodal, and usually symmetrical, peak. The microstructure of PLAs was determined by homodecoupling <sup>1</sup>H NMR spectroscopy at 20 °C in CDCl<sub>3</sub> on a Bruker AC-500 spectrometer.

**Crystal Structures Determination.** Diffraction data were collected at 100(2) K using a Bruker APEX CCD diffractometer with graphite-monochromatized MoK $\alpha$  radiation ( $\lambda = 0.71073 \text{ \AA}$ ). A combination of  $\omega$  and  $\phi$  scans was carried out to obtain at least a unique data set. The crystal structures were solved by direct methods, remaining atoms were located from difference Fourier synthesis followed by full-matrix least-squares refinement based on F2 (programs SIR97 and SHELXL-97)<sup>5</sup> with the aid of the WINGX program.<sup>6</sup> In most cases, many hydrogen atoms could be found from the Fourier difference analysis. Other hydrogen atoms were placed at calculated positions and forced to ride on the attached atom. The hydrogen atom contributions were calculated but not refined. All non-hydrogen atoms were refined with anisotropic displacement parameters. The locations of the largest peaks in the final difference Fourier map calculation as well as the magnitude of the residual electron densities were of no chemical significance. Crystal data and details of data collection and structure refinement for the different compounds are given in Annexes.

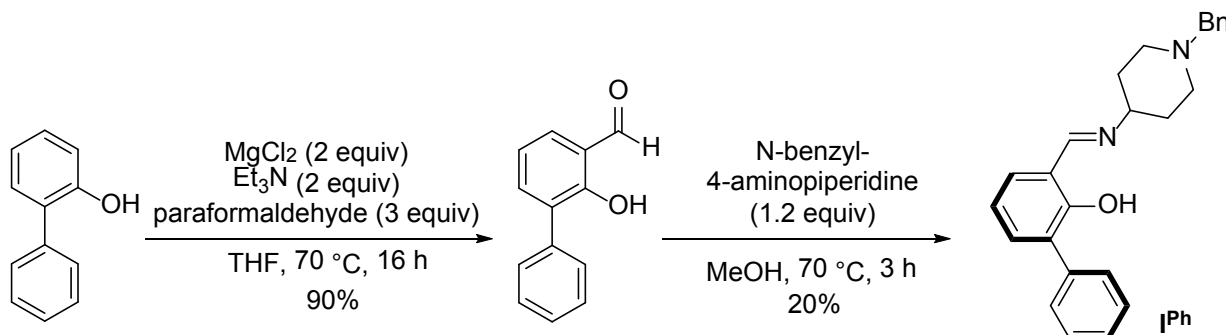
**[{ON<sup>pipeBn</sup>}H]<sub>2</sub> (II).** A solution of 2,9-dicarboxyaldehyde-1,8-bisphenol (1.00 g, 4.13 mmol), 4-amino-1-benzylpiperidine (2.30 g, 12.4 mmol) and PTSA (cat., *ca.* 2 mg) in benzene (20 mL) was stirred under reflux with a Dean-Stark apparatus at 120 °C for 48 h. Volatiles were removed under vacuum and the resulting solid recrystallized in methanol (*ca.* 20 mL). The resulting material was filtered, washed with cold methanol (30 mL) and dried *in vacuo* to give **II** as a yellow solid (2.03 g, 84%). <sup>1</sup>H NMR (500 MHz, C<sub>6</sub>D<sub>6</sub>, 298 K):  $\delta$  1.49 (m, 4H, CH<sub>2</sub> pip), 1.53-1.60 (m, 4H, CH<sub>2</sub> pip), 1.95 (m, 4H, CH<sub>2</sub> pip), 2.59 (m, 4H, CH<sub>2</sub> pip), 2.75 (m, 2H, CH

pip), 3.28 (s, 4H, NCH<sub>2</sub>Ph), 6.87 (t,  $J_{\text{H-H}} = 7.6$  Hz, 2H, Haro), 6.96-6.97 (dd,  $J_{\text{H-H}} = 1.7$  and 5.9 Hz, 2H, Haro), 7.10-7.13 (m, 2H, Haro), 7.21 (t,  $J_{\text{H-H}} = 7.6$  Hz, 4H, Haro), 7.33-7.34 (m, 4H, Haro), 7.70-7.71 (dd,  $^2J = 1.75$  and 5.7 Hz, 2H, Haro), 7.81 (s, 2H, ArCH=N), 14.10 (s, 2H, ArOH).  $^{13}\text{C}\{\text{H}\}$  NMR (125 MHz, C<sub>6</sub>D<sub>6</sub>, 298 K):  $\delta$  33.33 (CH<sub>2</sub> pip), 51.28 (CH<sub>2</sub> pip), 62.97 (NCH<sub>2</sub>Ph), 64.93 (CH pip), 117.60, 119.14, 126.54, 126.84, 128.15, 128.75, 130.58, 134.70, 139.32 (Caro), 159.56 (*ipso*-C phenol), 163.03 (ArCH=N). Anal. calcd. for C<sub>38</sub>H<sub>42</sub>N<sub>4</sub>O<sub>2</sub>: C, 77.78; H, 7.21; N, 9.55; found: C, 77.16; H, 7.26; N, 9.87. Mp: 253 °C.

**[{ON<sup>pipeBn</sup>}AlMe<sub>2</sub>]<sub>2</sub> (II-Al<sub>2</sub>).** A solution of [{ON<sup>pipeBn</sup>}H]<sub>2</sub> (II) (1.00 g, 1.70 mmol) in toluene (*ca.* 10 mL) was added to a solution of AlMe<sub>3</sub> (0.341 mL of a 1.0 M solution in *n*-heptane, 3.41 mmol) in toluene (*ca.* 10 mL). The reaction mixture was stirred at room temperature for 24 h. Then, volatiles were removed under vacuum and the resulting material washed with *n*-hexane (*ca.* 10 mL), and dried *in vacuo* to give II-Al<sub>2</sub> as a yellow solid (1.15 g, 96%).  $^1\text{H}$  NMR (500 MHz, C<sub>6</sub>D<sub>6</sub>, 298 K):  $\delta$  -0.29 (s, 12H, Al(CH<sub>3</sub>)<sub>2</sub>), 1.39 (m, 4H, CH<sub>2</sub> pip), 1.57 (td,  $J_{\text{H-H}} = 1.9$  and 9.9 Hz, 4H, CH<sub>2</sub> pip), 1.74-1.81 (qd,  $J_{\text{H-H}} = 3.5$  and 3.75 Hz, 4H, CH<sub>2</sub> pip), 2.62-2.64 (m, 4H, CH<sub>2</sub> pip), 2.74 (tt,  $J_{\text{H-H}} = 4.1$  and 12 Hz, 2H, CH pip), 3.25 (s, 4H, NCH<sub>2</sub>Ph), 6.66-6.72 (m, 4H, Haro), 7.10-7.13 (tt,  $J_{\text{H-H}} = 1.3$  and 7.3 Hz, 2H, Haro), 7.18-7.21 (m, 4H, Haro), 7.30-7.31 (m, 4H, Haro), 7.36 (s, 2H, ArCH=N), 7.87 (dd,  $J_{\text{H-H}} = 2.1$  and 5 Hz, 2H, Haro).  $^{13}\text{C}\{\text{H}\}$  NMR (125 MHz, C<sub>6</sub>D<sub>6</sub>, 298 K):  $\delta$  -7.91 (Al(CH<sub>3</sub>)<sub>2</sub>), 32.51 (CH<sub>2</sub> pip), 52.19 (CH<sub>2</sub> pip), 62.57 (NCH<sub>2</sub>Ph), 65.11 (CH pip), 116.55, 119.54, 127.09, 128.29, 128.73, 130.16, 134.10, 138.70, 139.30 (Caro), 162.18 (ArC-O-Al), 169.34 (ArCH=N). Anal. calcd. for C<sub>42</sub>H<sub>52</sub>Al<sub>2</sub>N<sub>4</sub>O<sub>2</sub>: C, 72.18; H, 7.50; N, 8.02; found: C, 72.52; H, 7.12; N, 8.22.

**[{ON<sup>pipeBn</sup>}In(CH<sub>2</sub>SiMe<sub>3</sub>)]<sub>2</sub> (II-In<sub>2</sub>).** A solution of [{ON<sup>pipeBn</sup>}H]<sub>2</sub> (II) (0.083 g, 0.142 mmol) in toluene (5 mL) and In(CH<sub>2</sub>SiMe<sub>3</sub>)<sub>3</sub> (0.117 g, 0.283 mmol) in toluene (2 mL) was stirred at 90 °C for 18 h. Then, volatiles were removed *in vacuo*, *n*-hexane (*ca.* 10 mL) was vacuum-condensed in and the resulting solution was filtered off. The filtrate was concentrated under vacuum to give II-In<sub>2</sub> as a bright yellow solid (0.092 g, 56%).  $^1\text{H}$  NMR (500 MHz,

C<sub>6</sub>D<sub>6</sub>, 298 K): δ -0.19 (d, <sup>2</sup>J<sub>H-H</sub> = 12.5 Hz, 4H, CHHSiMe<sub>3</sub>), -0.12 (d, <sup>2</sup>J<sub>H-H</sub> = 12.5 Hz, 4H, CHHSiMe<sub>3</sub>), 0.20 (s, 36H, Si(CH<sub>3</sub>)<sub>3</sub>), 1.43 (m, 4H, CH<sub>2</sub> pip), 1.65 (td, J<sub>H-H</sub> = 1.3 and 10.2 Hz, 4H, CH<sub>2</sub> pip), 1.77 (qd, J<sub>H-H</sub> = 3.5 and 12 Hz, 4H, CH<sub>2</sub> pip), 2.56 (tt, J<sub>H-H</sub> = 3.9 and 11.6 Hz, 2H, CH pip), 2.70 (m, 4 H, CH<sub>2</sub> pip), 3.28 (s, 4 H, NCH<sub>2</sub>Ph), 6.78 (t, J<sub>H-H</sub> = 7.8 Hz, 2H, Haro), 6.86-6.88 (dd, J<sub>H-H</sub> = 2.0 and 8.0 Hz, 2H, Haro), 7.09 (tt, J<sub>H-H</sub> = 1.8 and 7.3 Hz, 2H, Haro), 7.16-7.19 (m, 4H, Haro), 7.30 (m, 4H, Haro), 7.54 (s, 2H, CH=N), 7.91 (dd, J<sub>H-H</sub> = 2.0 and 7.2 Hz, 2H, Haro). <sup>13</sup>C{<sup>1</sup>H} NMR (125 MHz, C<sub>6</sub>D<sub>6</sub>, 298 K): δ 2.24 (CH<sub>2</sub>Si(CH<sub>3</sub>)<sub>3</sub>), 2.70 (Si(CH<sub>3</sub>)<sub>3</sub>), 34.07 (CH<sub>2</sub> pip), 52.05 (CH<sub>2</sub> pip), 62.74 (NCH<sub>2</sub>Ph), 68.92 (CH pip), 114.00, 118.74 127.12, 128.32, 128.80, 132.55, 135.31, 138.52, 138.61 (Caro), 167.84 (ArC–O–In), 169.86 (ArCH=N). Anal. calcd. for C<sub>54</sub>H<sub>84</sub>In<sub>2</sub>N<sub>4</sub>O<sub>2</sub>Si<sub>4</sub>: C, 55.76; H, 7.28; N, 4.82; found: C, 56.19 ; H, 7.37; N, 5.04.



**Scheme 1.** Synthetic route toward the phenol-imine pro-ligand (O<sup>Ph</sup>N<sup>pipeBn</sup>}H (I<sup>Ph</sup>).

**{ON<sup>pipeBn</sup>}<sup>Ph</sup>H (I<sup>Ph</sup>).** A solution of 2-hydroxybiphenyl-3-carbaldehyde (2.30 g, 11.7 mmol), N-benzyl-4-aminopiperidine (2.60 g, 13.9 mmol) in methanol (30 mL) was stirred [without catalyst] under reflux for 3 h. The reaction mixture was allowed to cool to room temperature, and volatiles were removed under vacuum till the apparition of a precipitate. The suspension was then stored at -30 °C for 24 h. The precipitate was filtered off, washed with cold methanol (3 × 20 mL) and dried *in vacuo* to give I<sup>Ph</sup> as a yellow solid (0.303 g, 20%). <sup>1</sup>H NMR

(400 MHz, C<sub>6</sub>D<sub>6</sub>, 298 K): δ 1.44-1.50 (m, 2H, CH<sub>2</sub> pip), 1.57-1.62 (m, 2H, CH<sub>2</sub> pip), 1.96 (t, J<sub>H-H</sub> = 9.2 Hz, 2H, CH<sub>2</sub> pip), 2.61-2.63 (m, 2H, CH<sub>2</sub> pip), 2.76 (m, 1H, CH pip), 3.31 (s, 2H, NCH<sub>2</sub>Ph), 6.80 (t, J<sub>H-H</sub> = 7.5 Hz, 1H, Haro), 6.91-6.93 (dd, J<sub>H-H</sub> = 1.6, 7.6 Hz, 1H, Haro), 7.21 (t, J<sub>H-H</sub> = 7.6 Hz, 2H, Haro), 7.28 (t, J<sub>H-H</sub> = 7.8 Hz, 2H, Haro), 7.33-7.37 (m, 3H, Haro), 7.80-7.81 (m, 3H, Haro and ArCH=N), 14.31 (s, 1H, ArOH). <sup>13</sup>C{<sup>1</sup>H} NMR (100 MHz, C<sub>6</sub>D<sub>6</sub>, 298 K): δ 33.33 (CH<sub>2</sub> pip), 51.29 (CH<sub>2</sub> pip), 62.99 (NCH<sub>2</sub>Ph), 64.97 (CH pip), 118.24, 119.23, 128.77, 129.64, 130.51, 130.51, 133.14, 138.21, 139.19 (Caro), 159.10 (*ipso*-C phenol), 163.00 (ArCH=N). Anal. calcd. C<sub>25</sub>H<sub>26</sub>N<sub>2</sub>O: C, 81.05; H, 7.07; N, 7.56; found: C, 80.88; H, 7.10; N, 7.49.

**{ON<sup>pipeBn</sup>}<sup>Ph</sup>AlMe<sub>2</sub> (**I<sup>Ph</sup>-Al**).** A solution of {ON<sup>pipeBn</sup>}<sup>Ph</sup>H (**I<sup>Ph</sup>**) (0.053 g, 0.140 mmol) in toluene (*ca.* 3 mL) was added to a solution of AlMe<sub>3</sub> (0.140 mL of a 1.0 M solution in *n*-heptane, 0.140 mmol) in toluene (*ca.* 3 mL). The reaction mixture was stirred at room temperature for 18 h. Then, volatiles were removed under vacuum and the resulting material washed with *n*-hexane (*ca.* 5 mL), and dried *in vacuo* to give **I<sup>Ph</sup>-Al** as a yellow solid (0.042 g, 70%). <sup>1</sup>H NMR (400 MHz, C<sub>6</sub>D<sub>6</sub>, 298 K): δ -0.47 (s, 6H, Al(CH<sub>3</sub>)<sub>2</sub>), 1.22 (m, 2H, CH<sub>2</sub>pip), 1.43 (t, <sup>3</sup>J<sub>H-H</sub> = 10.8 Hz, 2H, CH<sub>2</sub> pip), 1.62 (m, 2H, CH<sub>2</sub> pip), 2.47 (m, 2H, CH<sub>2</sub> pip), 2.61 (m, 1H, CH pip), 3.11 (s, 2H, NCH<sub>2</sub>Ph), 6.49 (t, J<sub>H-H</sub> = 7.6 Hz, 1H, Haro), 6.57 (m, 1H, Haro), 6.64 (m, 2H, Haro), 7.04-7.16 (m, 6H, Haro), 7.26 (s, 1H, Haro), 7.28 (s, 1H, ArCH=N), 7.60 (s, 1H, Haro), 7.62 (s, 1H, Haro). <sup>13</sup>C{<sup>1</sup>H} NMR (100 MHz, C<sub>6</sub>D<sub>6</sub>, 298 K): δ -9.17 (Al(CH<sub>3</sub>)<sub>2</sub>), 31.47 (CH<sub>2</sub> pip), 51.10 (CH<sub>2</sub> pip), 61.51 (NCH<sub>2</sub>Ph), 64.31 (NCH pip), 116.05, 118.51, 127.27, 128.39, 132.74, 132.91, 136.45, 137.37, 137.57 (Caro), 160.76 (ArC-O-Al), 168.20 (ArCH=N). Anal. calcd. C<sub>27</sub>H<sub>31</sub>AlN<sub>2</sub>O: C, 76.03; H, 7.33; N, 6.57; found: C, 76.35; H, 7.49; N, 6.51.

**General Procedure for Kinetic Studies of ROP of racemic Lactide.** Each polymerization experiment was conducted in a Teflon valve-sealed Schlenk flask as previously described. After a given time period, the reaction was quenched with H<sub>2</sub>O (*ca.* 0.5 mL of a 10

wt% H<sub>2</sub>O solution in THF). The monomer (LA) conversion was calculated from <sup>1</sup>H NMR spectra of the crude reaction mixture in CDCl<sub>3</sub>, from the integration (Int.) ratio Int.<sub>polymer</sub>/[Int.<sub>polymer</sub>+Int.<sub>monomer</sub>], using the methyl hydrogen resonances for PLA at δ 1.49 ppm and for LA at δ 1.16 ppm. Then, the polymer was separated from the crude reaction mixture by filtration and was re-precipitated 3 times with excess pentane (*ca.* 15 mL). The polymer was then dried under vacuum till constant weight.

The microstructure of PLAs was determined by homodecoupling <sup>1</sup>H NMR spectroscopy (methine region) at 20 °C in CDCl<sub>3</sub> on a Bruker AC-500 spectrometer.

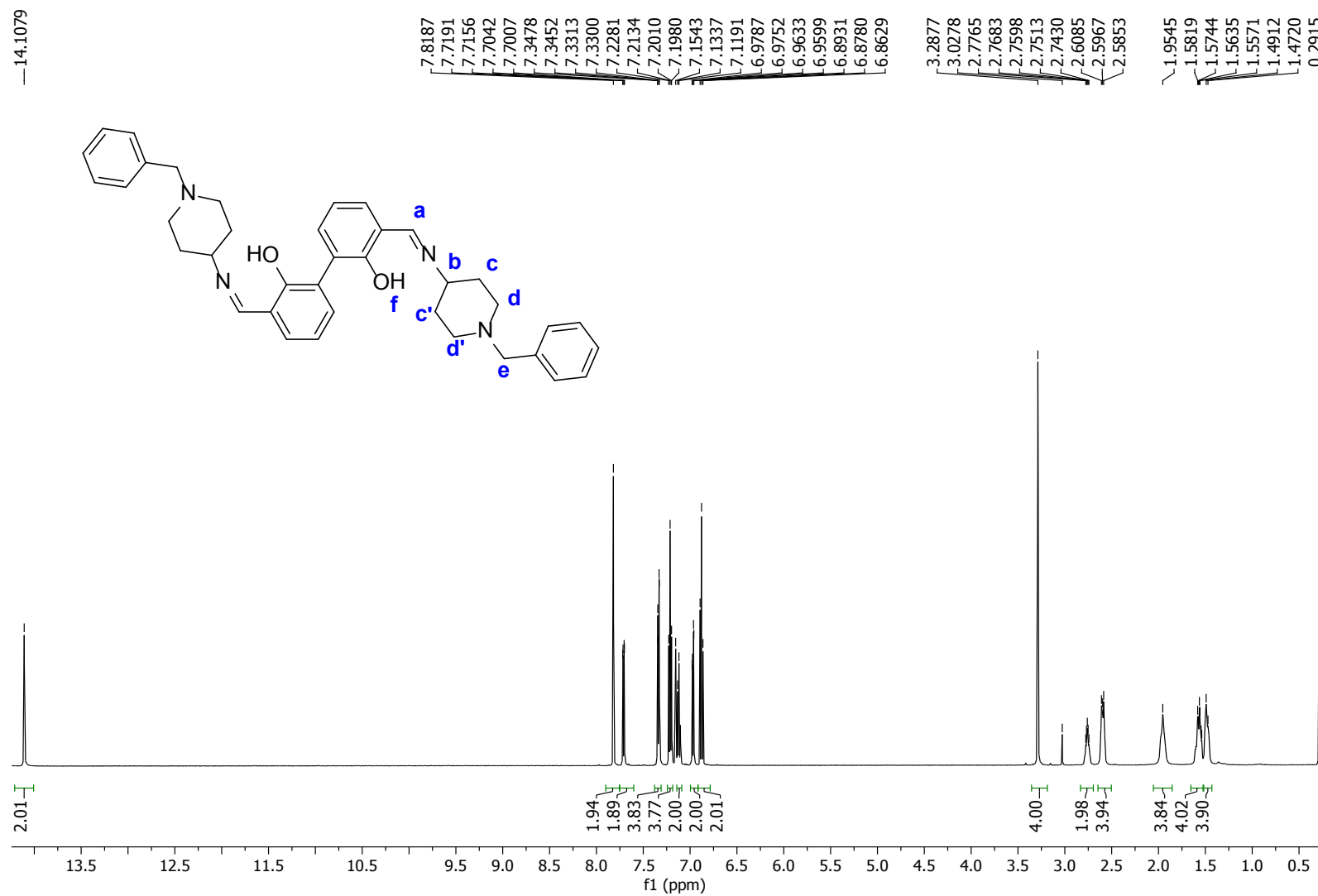


**Figure S1.**  $^1\text{H}$  NMR spectrum (500 MHz,  $\text{C}_6\text{D}_6$ , 298 K) of  $\text{[ON}^{\text{pipeBn}}\text{H}]_2$  (**II**). \* stands for grease.

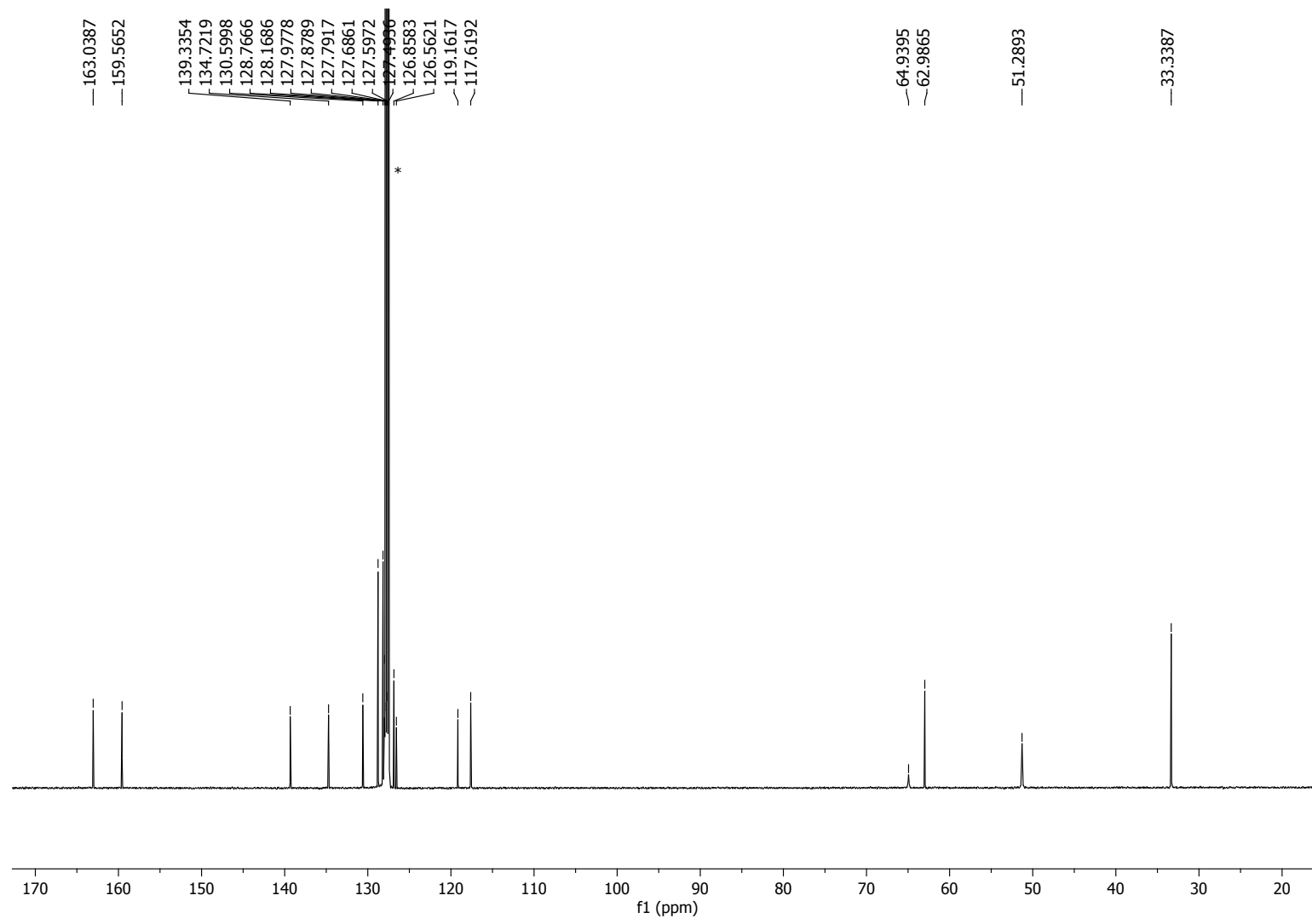


**Figure S2.**  $^{13}\text{C}\{^1\text{H}\}$  NMR spectrum (125 MHz,  $\text{C}_6\text{D}_6$ , 298 K) of  $[\{\text{ON}^{\text{pipeBn}}\}\text{H}]_2$  (**II**). \* stands for residual signal of  $\text{C}_6\text{D}_6$ .

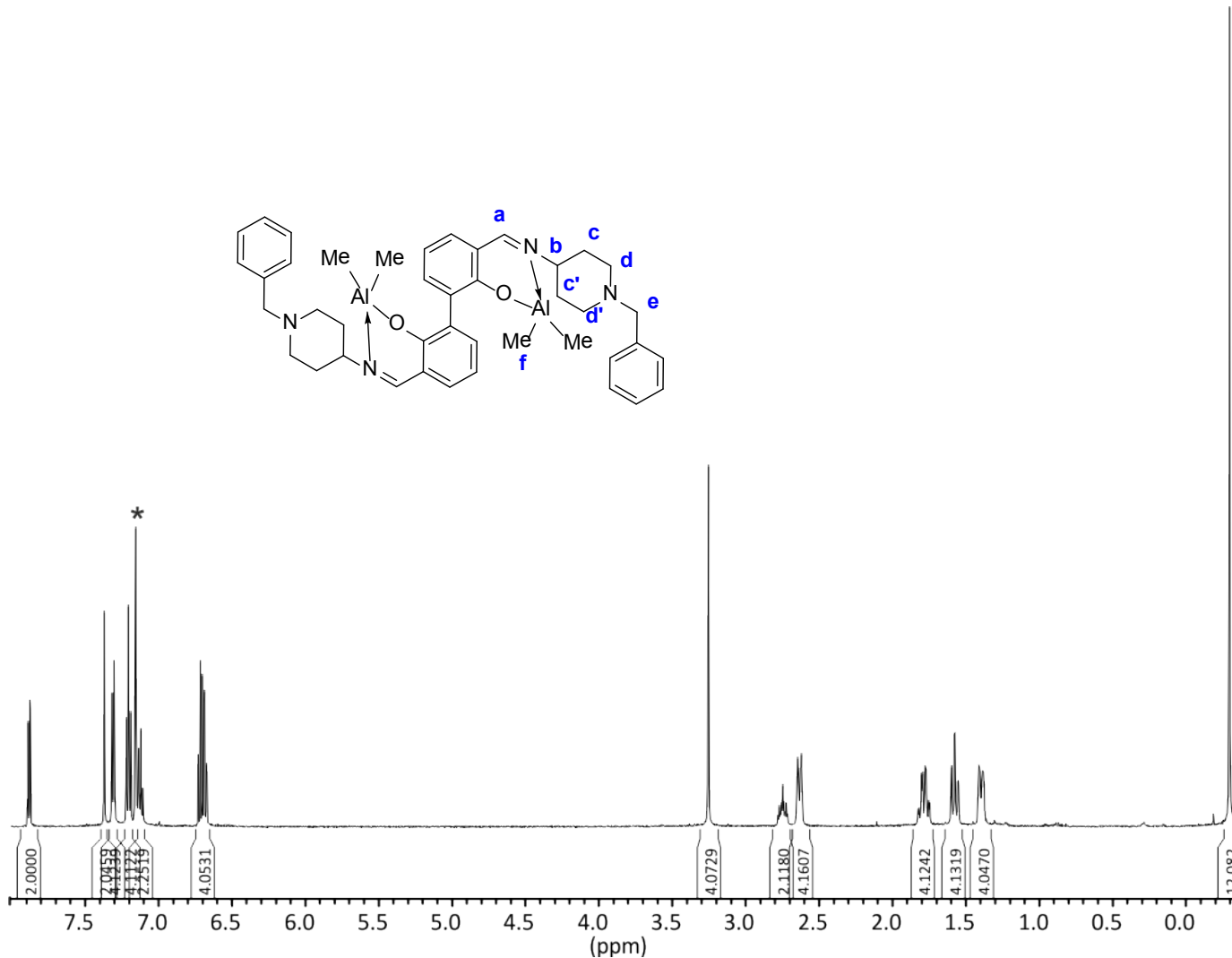


**Figure S3.** <sup>1</sup>H NMR spectrum (500 MHz, C<sub>6</sub>D<sub>6</sub>, 298 K) of [{ON<sup>pipeBn</sup>}AlMe<sub>2</sub>]<sub>2</sub> (**II-Al<sub>2</sub>**). \* stands for grease.

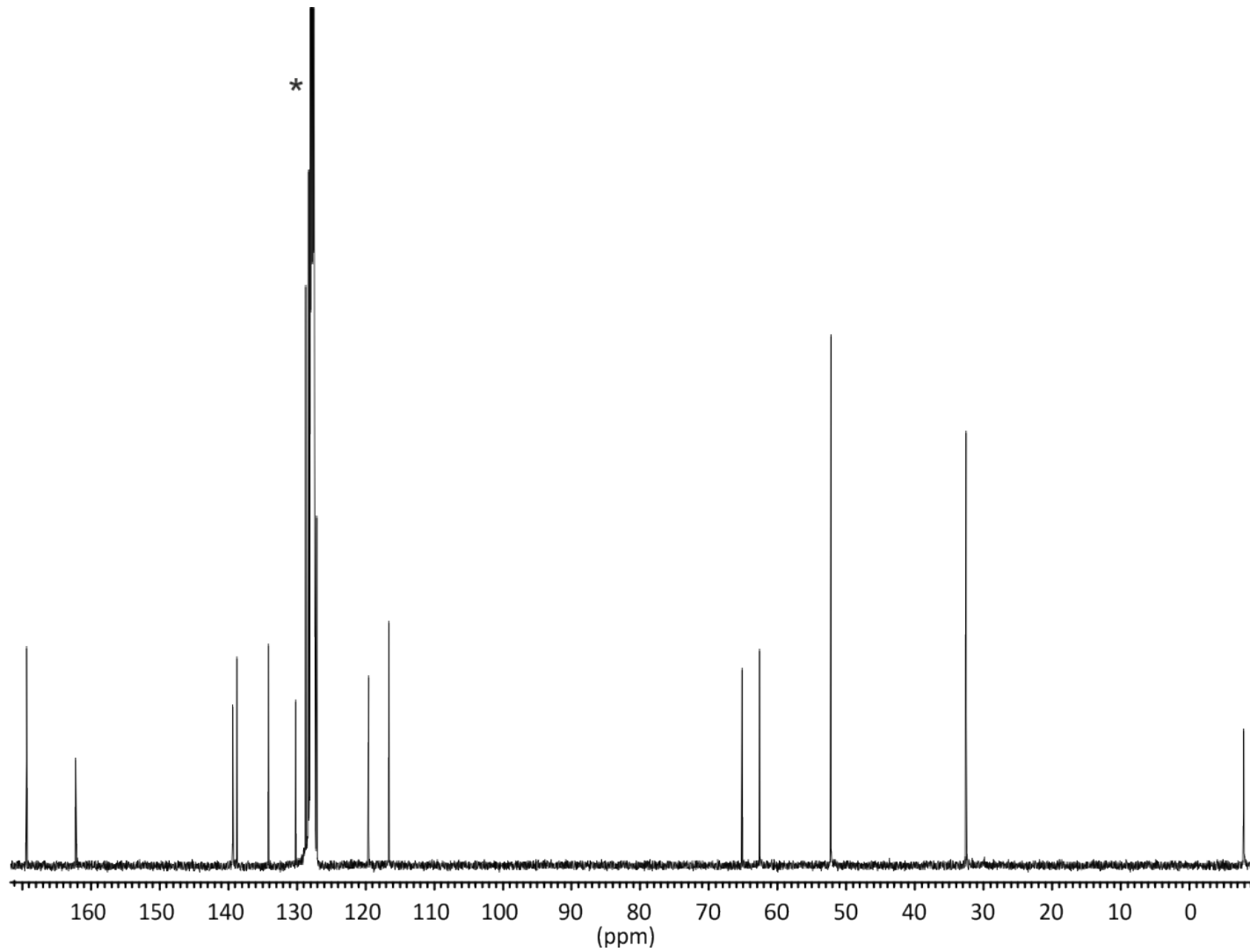


**Figure S4.**  $^{13}\text{C}\{^1\text{H}\}$  NMR spectrum (125 MHz,  $\text{C}_6\text{D}_6$ , 298 K) of  $[\{\text{ON}^{\text{pipeBn}}\}\text{AlMe}_2]_2$  (**II–Al<sub>2</sub>**). \* stands for residual signal of  $\text{C}_6\text{D}_6$ .

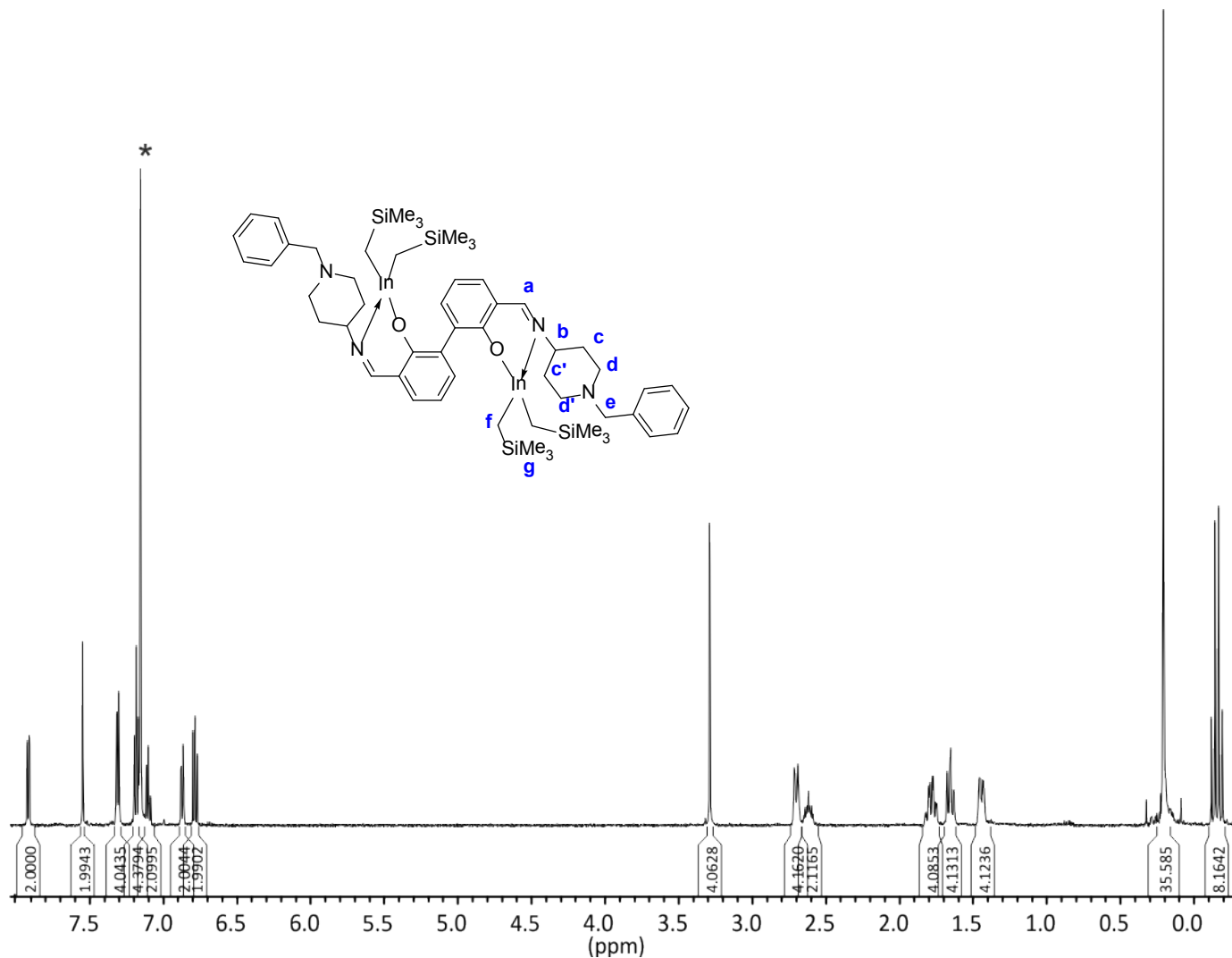


**Figure S5.**  $^1\text{H}$  NMR spectrum (500 MHz,  $\text{C}_6\text{D}_6$ , 298 K) of  $[\{\text{ON}^{\text{pipeBn}}\}\text{In}(\text{CH}_2\text{SiMe}_3)_2]_2$  (**II–In<sub>2</sub>**). \* stands for signal of residual  $\text{C}_6\text{D}_6$ .

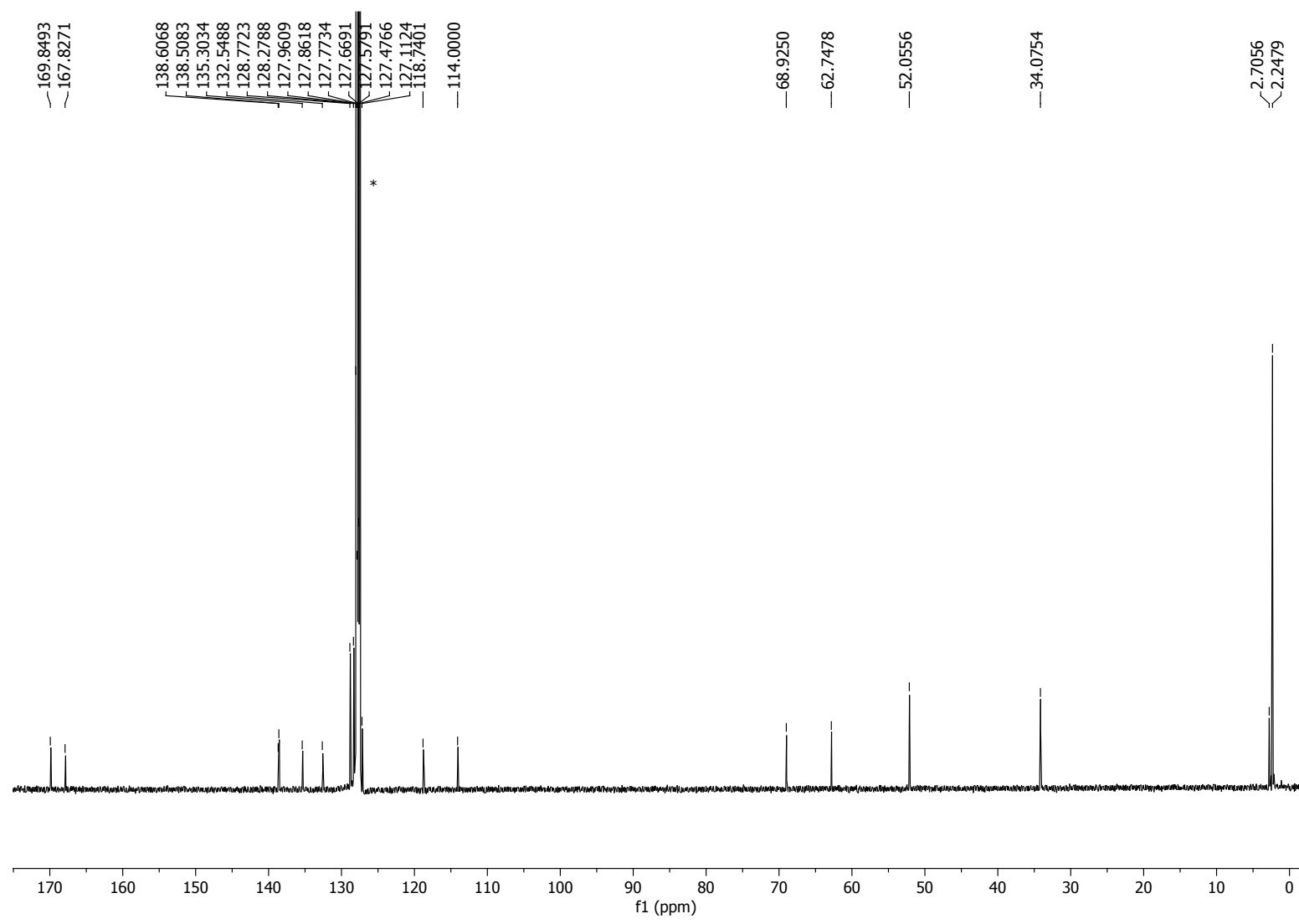


**Figure S6.**  $^{13}\text{C}\{^1\text{H}\}$  NMR spectrum (125 MHz,  $\text{C}_6\text{D}_6$ , 298 K) of  $[\{\text{ON}^{\text{pipeBn}}\}\text{In}(\text{CH}_2\text{SiMe}_3)_2]_2$  (**II–In<sub>2</sub>**). \* stands for residual signal of  $\text{C}_6\text{D}_6$ .

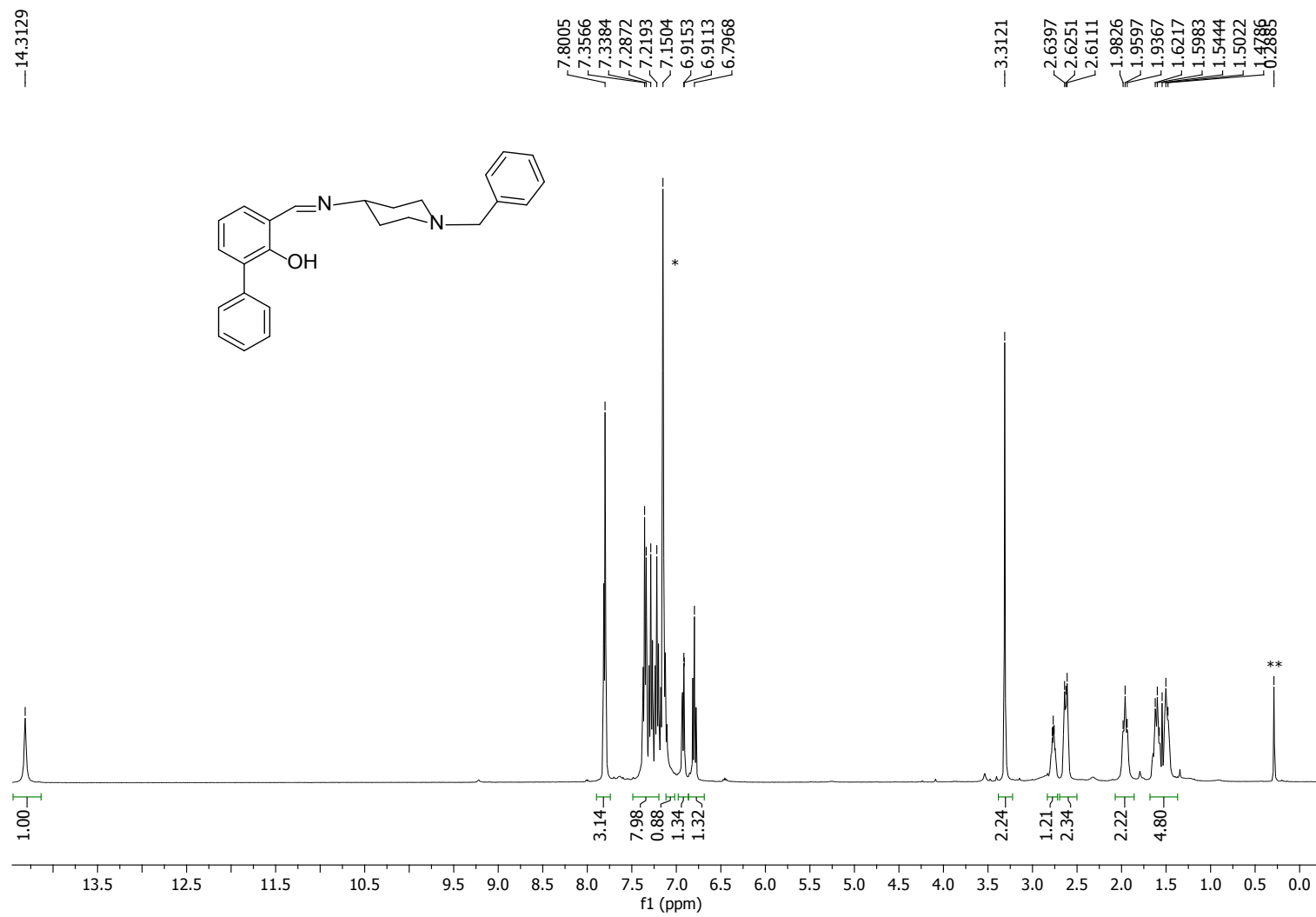


**Figure S7.** <sup>1</sup>H NMR spectrum (400 MHz, C<sub>6</sub>D<sub>6</sub>, 298 K) of  $\{\text{ON}^{\text{pipeBn}}\}^{\text{Ph}}\text{H}$  ( $\mathbf{I}^{\text{Ph}}$ ). \* and \*\* stand for signals of residual C<sub>6</sub>D<sub>6</sub> and grease, respectively.

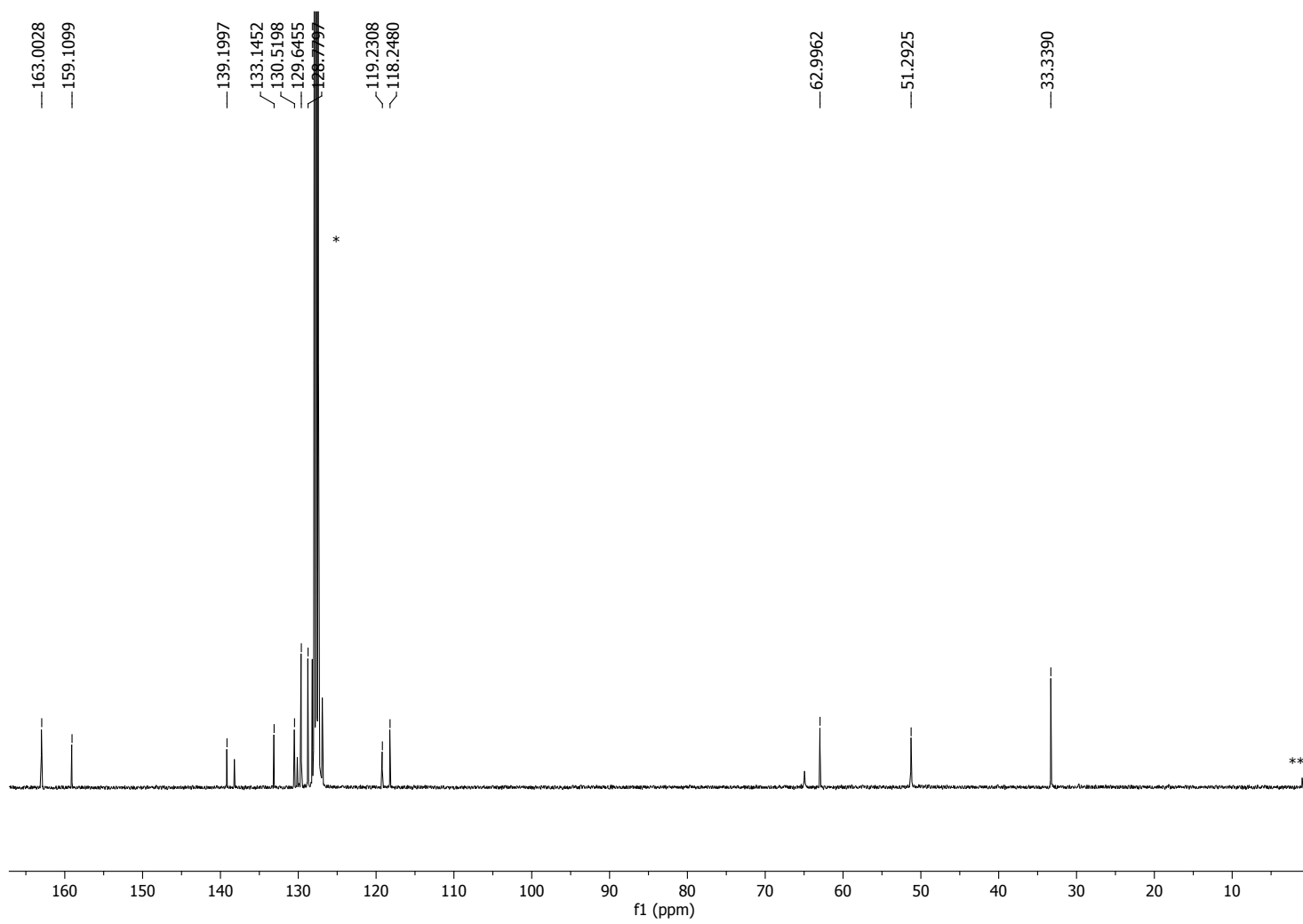


**Figure S8.**  $^{13}\text{C}\{\text{H}\}$  NMR spectrum (100 MHz,  $\text{C}_6\text{D}_6$ , 298 K) of  $\{\text{ON}^{\text{pipeBn}}\}^{\text{Ph}}\text{H}$  ( $\text{I}^{\text{Ph}}$ ). \* and \*\* stand for signals of residual  $\text{C}_6\text{D}_6$  and grease, respectively.

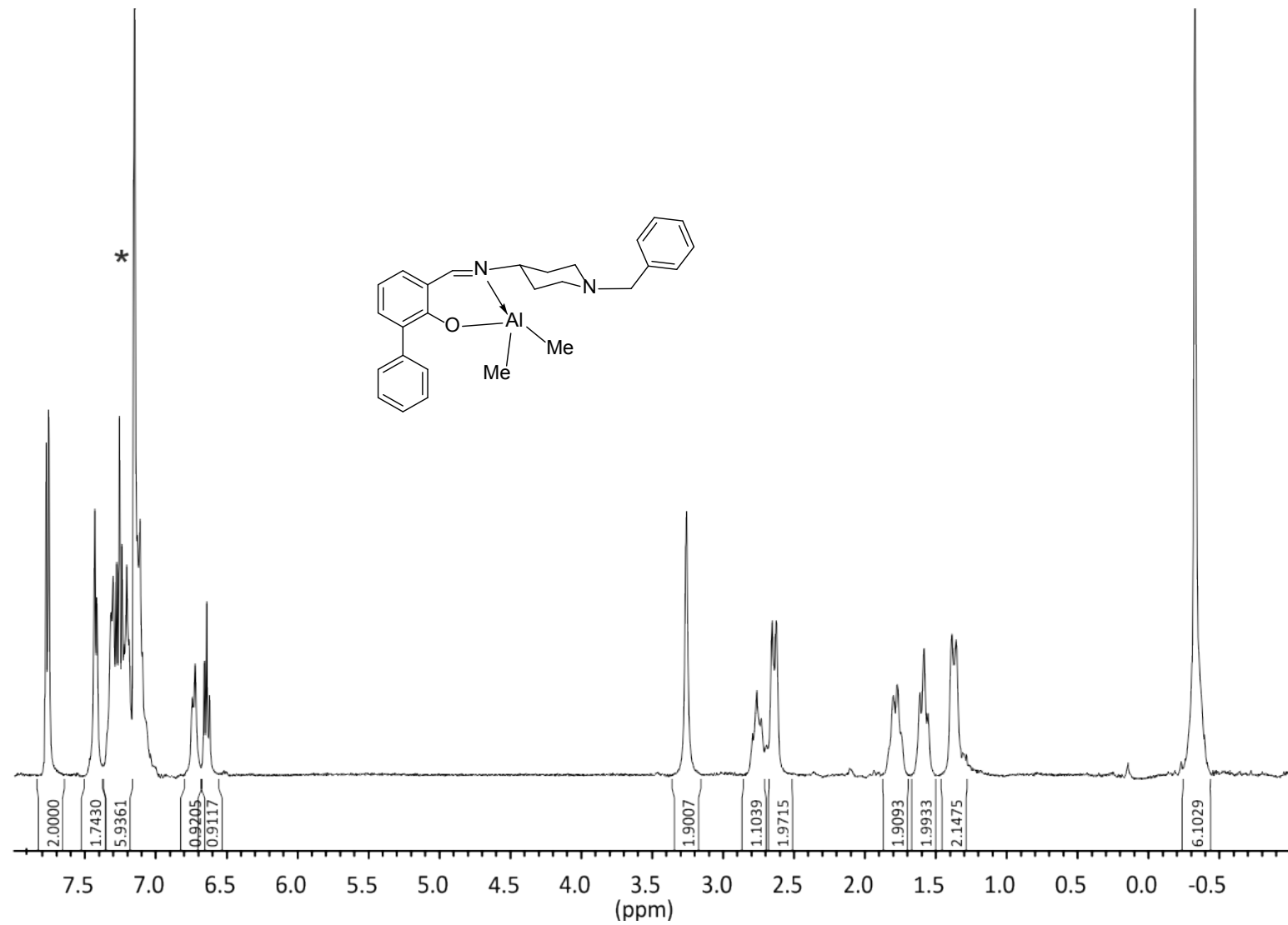


**Figure S9.**  $^1\text{H}$  NMR spectrum (400 MHz,  $\text{C}_6\text{D}_6$ , 298 K) of  $\{\text{ON}^{\text{pipeBn}}\}_{\text{Ph}}^{\text{AlMe}_2}$  ( $\text{I}^{\text{Ph}}-\text{Al}$ ). \* stands for signal of  $\text{C}_6\text{D}_6$ .

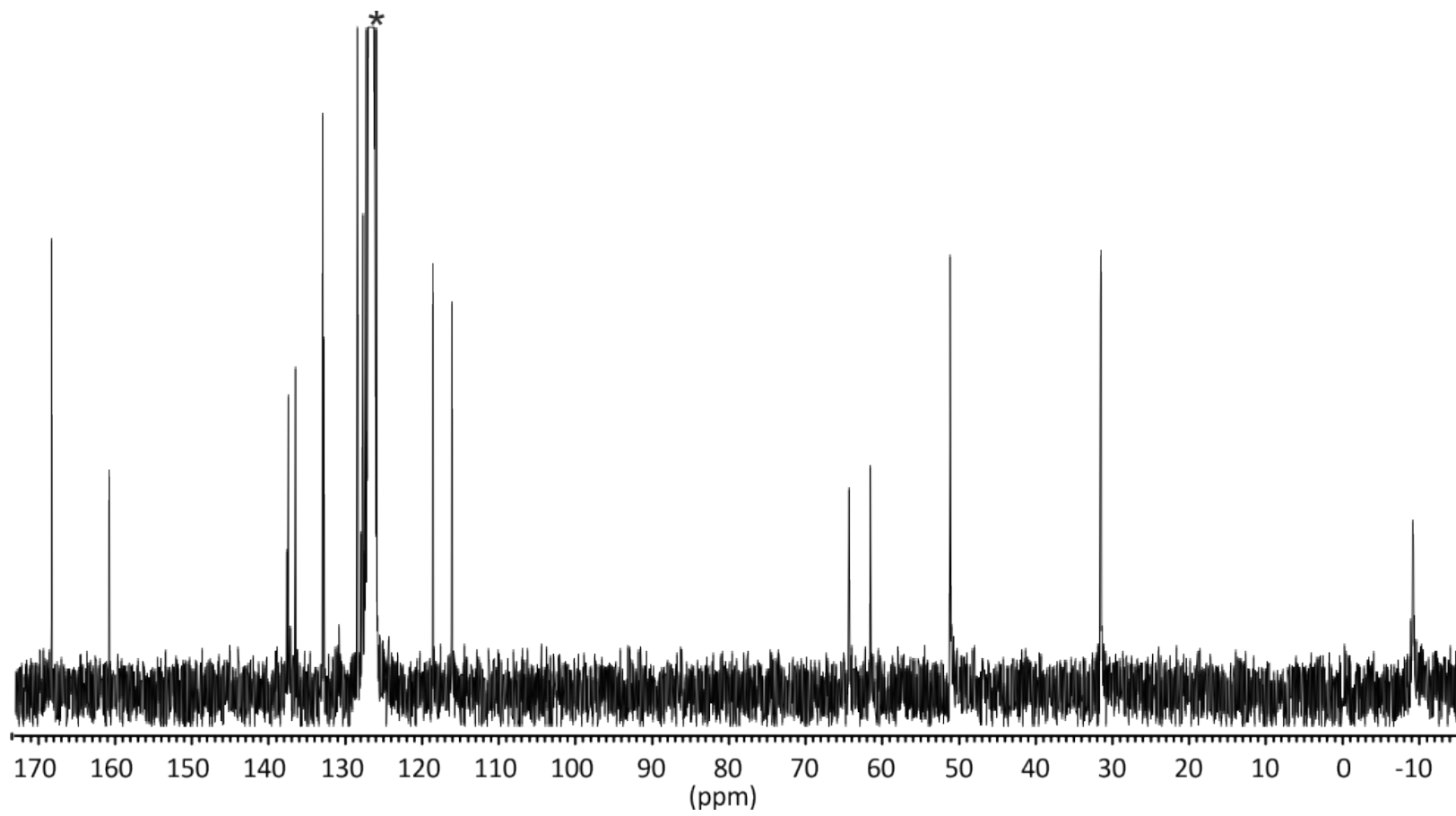


**Figure S10.**  $^{13}\text{C}\{^1\text{H}\}$  NMR spectrum (100 MHz,  $\text{C}_6\text{D}_6$ , 298 K) of  $\{\text{ON}^{\text{pipeBn}}\}^{\text{Ph}}\text{AlMe}_2$  ( $\mathbf{I}^{\text{Ph}}\text{-Al}$ ). \* stands for signal of  $\text{C}_6\text{D}_6$ .

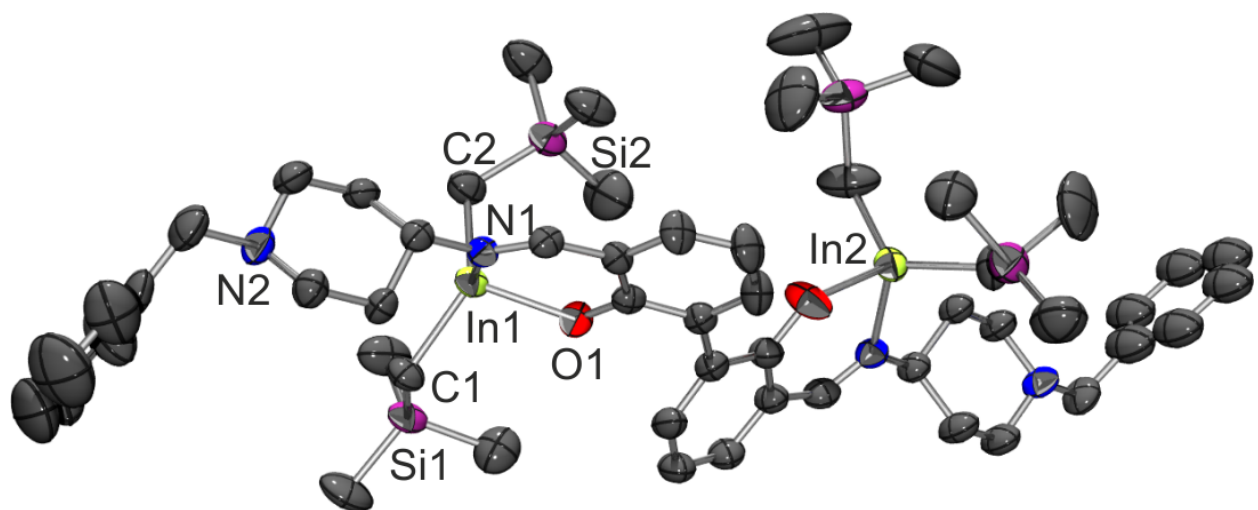


**Figure S11.** Molecular structure of the dinuclear complex **II-In<sub>2</sub>** (all hydrogen atoms are omitted for clarity; ellipsoids drawn at 50% level).

**Table S1.** Summary of Crystal and Refinement Data for Complexes **II-Al<sub>2</sub>** and **II-In<sub>2</sub>**.

	<b>II-Al<sub>2</sub></b>	<b>II-In<sub>2</sub></b>
Empirical formula	C <sub>336</sub> H <sub>416</sub> Al <sub>16</sub> N <sub>32</sub> O <sub>16</sub>	C <sub>54</sub> H <sub>84</sub> In <sub>2</sub> N <sub>4</sub> O <sub>2</sub> Si <sub>4</sub>
Formula weight	5590.69	1163.25
Crystal system	Orthorhombic	Triclinic
Space group	F 2 d d	<i>P</i> -1
<i>a</i> , Å	15.3906(12)	10.335(3)
<i>b</i> , Å	41.213(3)	14.576(4)
<i>c</i> , Å	55.854(4)	20.959(6)
α, deg	90	95.297(13)
β, deg	90	99.709(11)
γ, deg	90	95.859(12)
Volume, Å <sup>3</sup>	35428(5)	3076.5(15)
Z	4	2
Density, g.m <sup>-3</sup>	1.048	1.256
Abs. coeff., mm <sup>-1</sup>	0.101	0.866
F(000)	11968	1212
Crystal size, mm	0.6 x 0.09 x 0.08	0.6 x 0.3 x 0.13
θ range, deg	1.23 to 27.54 -20 ≤ <i>h</i> ≤ 13, -53 ≤ <i>k</i> ≤ 53, -72 ≤ <i>l</i> ≤ 72	2.92 to 27.62 -13 ≤ <i>h</i> ≤ 9, -18 ≤ <i>k</i> ≤ 18, -27 ≤ <i>l</i> ≤ 27
Limiting indices		
Reflec. Collected	76390	34709
Refle. Unique [I>2σ(I)]	18553 (17458)	13984 (9503)
Data/restrains/ param.	18553 / 1 / 909	13984 / 0 / 575
Goodness-of-fit on F <sup>2</sup>	0.925	1.021
R <sub>1</sub> [I>2σ(I)] (all data)	0.0686 (0.1326)	0.044 (0.0894)
wR <sub>2</sub> [I>2σ(I)] (all data)	0.1463 (0.1677)	0.0763 (0.1028)
Largest diff. e.A <sup>-3</sup>	0.622 and -0.313	1.458 and -0.863

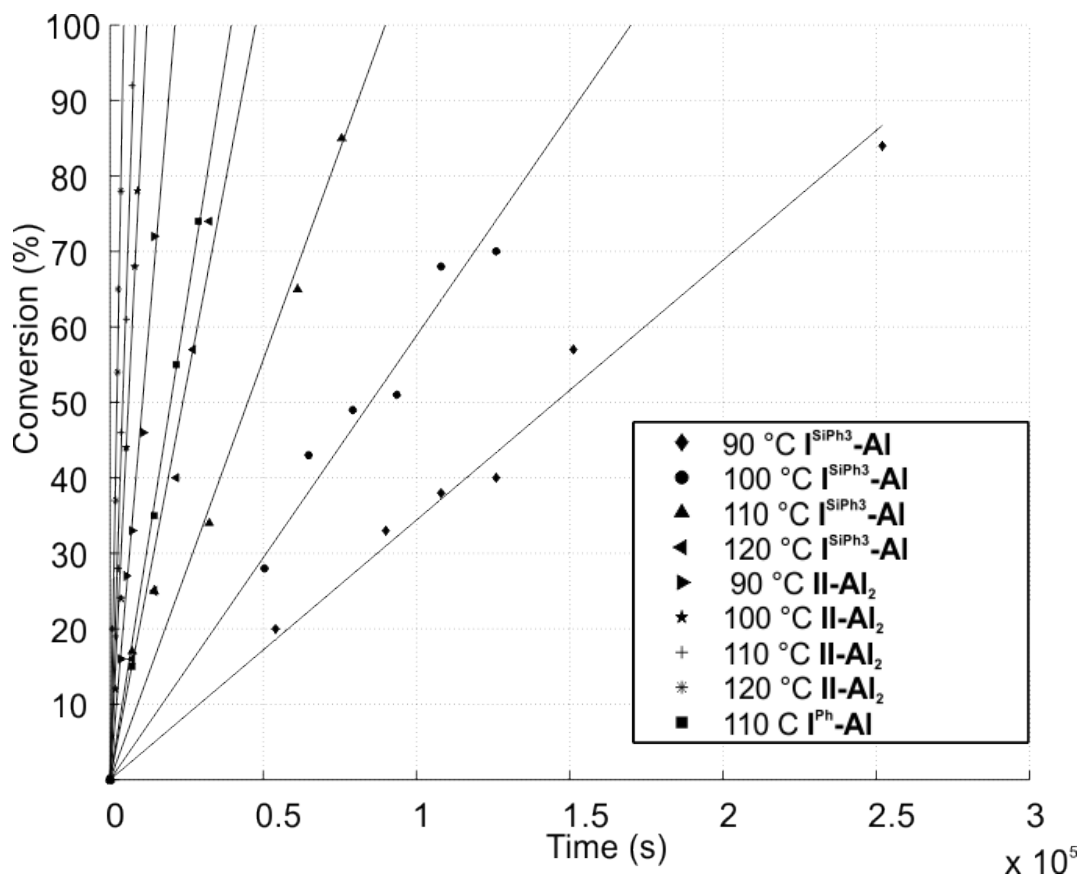


**Figure S12.** Plot of *rac*-LA conversion (%) vs. time (s) for the binary system [Al]/iPrOH at different temperatures: (a) mononuclear systems; conditions: toluene,  $[rac\text{-LA}]_0/[Al]/[i\text{PrOH}]_0 = 500:1:5$  ( $[rac\text{-LA}]_0 = 2.0 \text{ M}$ ;  $[Al]_0 = 4.0 \text{ mM}$ ;  $[i\text{PrOH}]_0 = 20 \text{ mM}$ ). **I**<sup>SiPh<sub>3</sub></sup>**-Al**: ◆ — 90 °C,  $k_{\text{app}} = 3.4 \pm 0.2 \cdot 10^{-4} \text{ s}^{-1}$ ,  $R^2 = 0.964$ ; ● — 100 °C,  $k_{\text{app}} = 5.9 \pm 0.4 \cdot 10^{-4} \text{ s}^{-1}$ ,  $R^2 = 0.976$ ; ▲ — 110 °C,  $k_{\text{app}} = 1.1 \pm 0.2 \cdot 10^{-3} \text{ s}^{-1}$ ,  $R^2 = 0.965$ ; ◀ — 120 °C,  $k_{\text{app}} = 2.1 \pm 0.2 \cdot 10^{-3} \text{ s}^{-1}$ ,  $R^2 = 0.975$ . **I**<sup>Ph</sup>**-Al**: ■ — 110 °C,  $k_{\text{app}} = 2.5 \pm 0.1 \cdot 10^{-3} \text{ s}^{-1}$ ,  $R^2 = 0.996$ ; (b) dinuclear system; conditions: toluene,  $[rac\text{-LA}]_0/[Al]/[i\text{PrOH}]_0 = 1000:2:10$  ( $[rac\text{-LA}]_0 = 2.0 \text{ M}$ ;  $[Al]_0 = 4.0 \text{ mM}$ ;  $[i\text{PrOH}]_0 = 20 \text{ mM}$ ). **II-Al<sub>2</sub>**: ► — 90 °C,  $k_{\text{app}} = 4.7 \pm 0.4 \cdot 10^{-3} \text{ s}^{-1}$ ,  $R^2 = 0.985$ ; ★ — 100 °C,  $k_{\text{app}} = 8.3 \pm 0.6 \cdot 10^{-3} \text{ s}^{-1}$ ,  $R^2 = 0.989$ ; + — 110 °C,  $k_{\text{app}} = 1.2 \pm 0.1 \cdot 10^{-2} \text{ s}^{-1}$ ,  $R^2 = 0.985$ ; \* — 120 °C,  $k_{\text{app}} = 2.2 \pm 0.2 \cdot 10^{-2} \text{ s}^{-1}$ ,  $R^2 = 0.987$ .

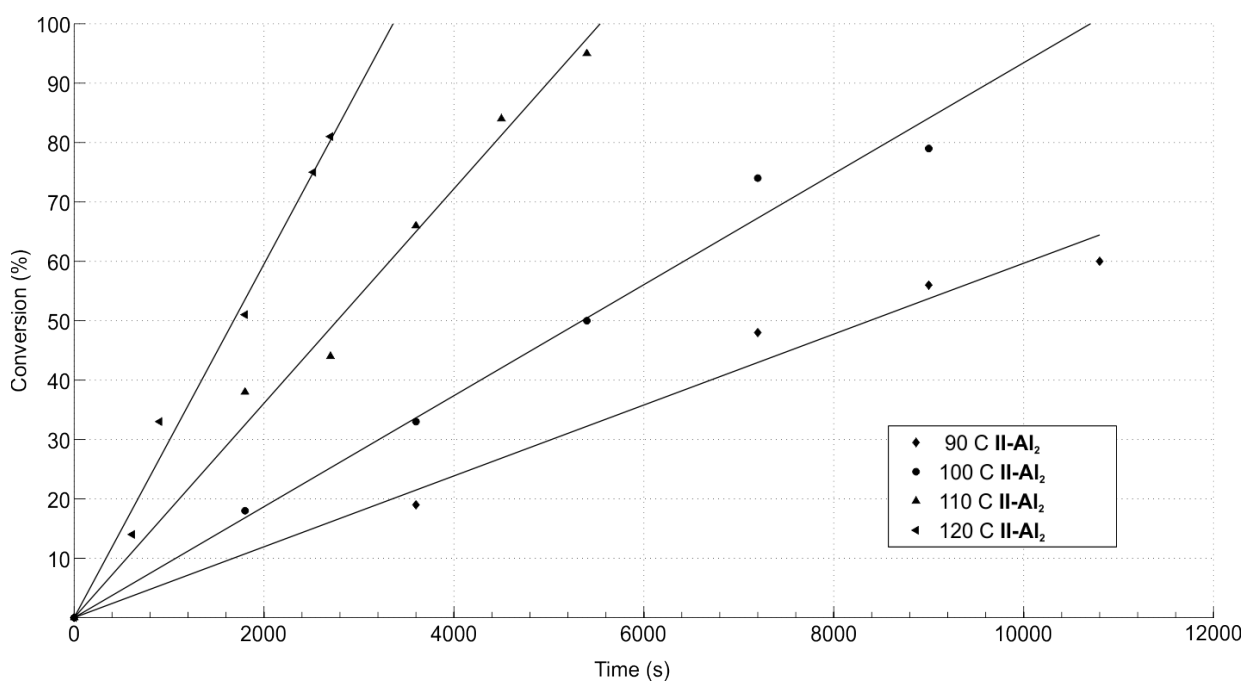


**Figure S13.** Plot of *rac*-LA conversion (%) vs. time (s) for the binary system **II–Al<sub>2</sub>/iPrOH** at different temperatures: conditions: toluene,  $[rac\text{-LA}]_0/[Al]/[i\text{PrOH}]_0 = 1000:4:10$  ( $[rac\text{-LA}]_0 = 2.0 \text{ M}$ ;  $[Al]_0 = 8.0 \text{ mM}$ ;  $[i\text{PrOH}]_0 = 20 \text{ mM}$ ). ♦ — 90 °C,  $k_{\text{app}} = 6.0 \pm 0.6 \cdot 10^{-3} \text{ s}^{-1}$ ,  $R^2 = 0.979$ ; • — 100 °C,  $k_{\text{app}} = 9.3 \pm 0.7 \cdot 10^{-3} \text{ s}^{-1}$ ,  $R^2 = 0.985$ ; ▲ — 110 °C,  $k_{\text{app}} = 1.8 \pm 0.1 \cdot 10^{-2} \text{ s}^{-1}$ ,  $R^2 = 0.989$ ; ◀ — 120 °C,  $k_{\text{app}} = 3.0 \pm 0.2 \cdot 10^{-2} \text{ s}^{-1}$ ,  $R^2 = 0.988$ .

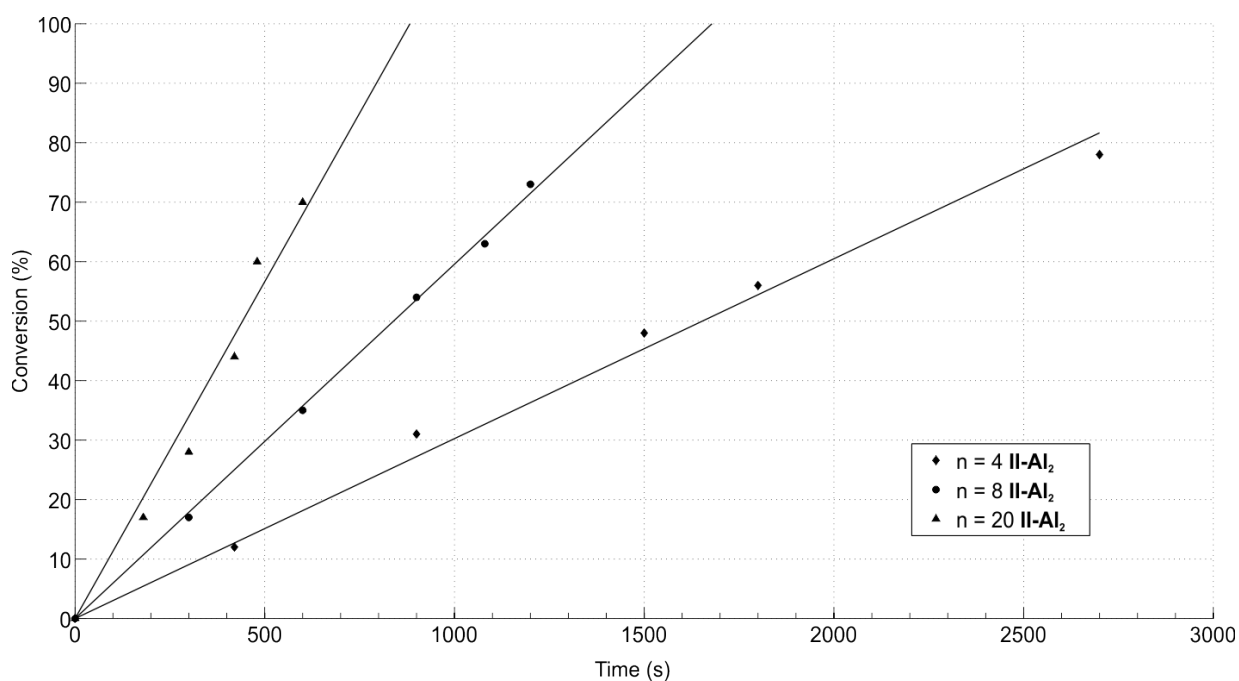


**Figure S14.** Plot of *rac*-LA conversion (%) vs. time (s) at 110 °C, at different concentrations of catalyst/initiator, with the binary system **II–Al<sub>2</sub>**/iPrOH. Conditions: toluene,  $[rac\text{-LA}]_0/[Al]/[i\text{PrOH}]_0 = 1000:n:50$  ( $[rac\text{-LA}]_0 = 2.0 \text{ M}$ ;  $[i\text{PrOH}]_0 = 100 \text{ mM}$ ). ◆ —  $n = 4$  ( $[Al]_0 = 8.0 \text{ mM}$ ),  $k_{\text{app}} = 3.0 \pm 0.2 \cdot 10^{-2} \text{ s}^{-1}$ ,  $R^2 = 0.991$ ; ● —  $n = 8$  ( $[Al]_0 = 16.0 \text{ mM}$ ),  $k_{\text{app}} = 6.0 \pm 0.1 \cdot 10^{-2} \text{ s}^{-1}$ ,  $R^2 = 0.999$ ; ▲ —  $n = 20$  ( $[Al]_0 = 40.0 \text{ mM}$ ),  $k_{\text{app}} = 1.1 \pm 0.1 \cdot 10^{-1} \text{ s}^{-1}$ ,  $R^2 = 0.973$ .

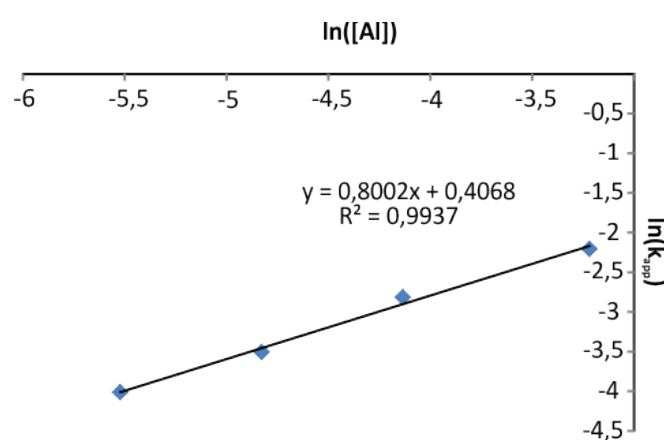


**Figure S15.** Plot of  $\ln(k_{\text{app}})$  vs.  $\ln([Al])$  for ROP of *rac*-LA by the binary system **II–Al<sub>2</sub>**/iPrOH at 110 °C,  $[rac\text{-LA}]_0 = 2.0 \text{ M}$ ,  $[i\text{PrOH}]_0 = 100 \text{ mM}$  in toluene and  $[Al]_0 = 4.0 \text{ mM}$ , 8.0 mM, 16.0 mM and 40.0 mM.

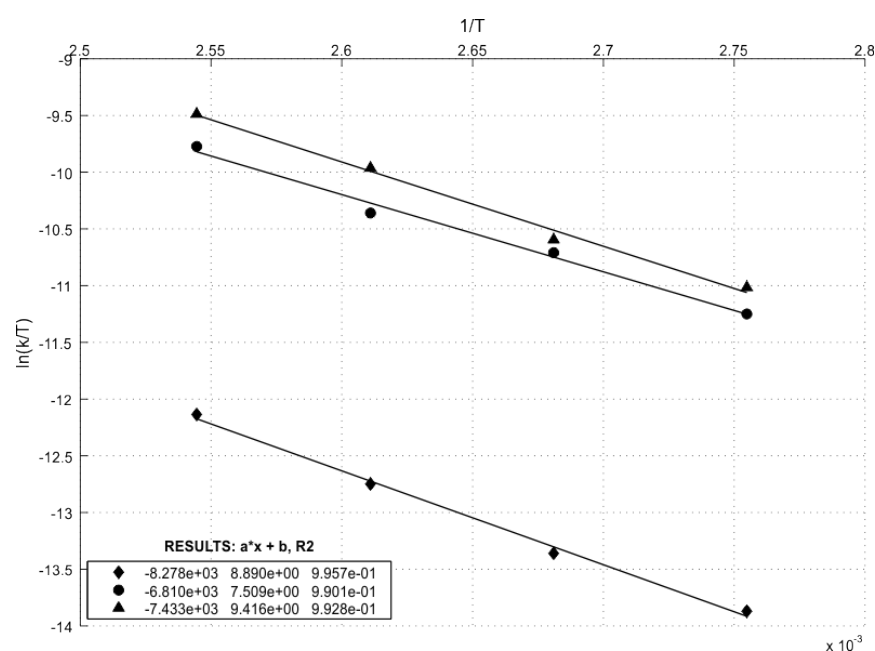


**Figure S16.** Plot of  $\ln(k_{\text{app}}/T)$  vs.  $1/T$  for ROP of *rac*-LA by the binary systems  $\mathbf{I}^{\text{SiPh3}}\text{-Al}$  and  $\mathbf{II}\text{-Al}_2/i\text{PrOH}$ ,  $[\text{rac-LA}]_0 = 2.0$  M in toluene. ◆ —  $\mathbf{I}^{\text{SiPh3}}\text{-Al}$ ;  $\Delta H^\ddagger = 16.4(1)$  kcal·mol<sup>-1</sup>,  $\Delta S^\ddagger = -29(4)$  cal·mol<sup>-1</sup>·K<sup>-1</sup>,  $\Delta G^\ddagger_{298} = 25.2(1)$  kcal·mol<sup>-1</sup>,  $R^2 = 0.996$ . ● —  $\mathbf{II}\text{-Al}_2$  (1000:2:10);  $\Delta H^\ddagger = 13.5(1)$  kcal·mol<sup>-1</sup>,  $\Delta S^\ddagger = -32(5)$  cal·mol<sup>-1</sup>·K<sup>-1</sup>,  $\Delta G^\ddagger_{298} = 23.1(1)$  kcal·mol<sup>-1</sup>,  $R^2 = 0.990$ . ▲ —  $\mathbf{II}\text{-Al}_2$  (1000:4:10);  $\Delta H^\ddagger = 14.8(1)$  kcal·mol<sup>-1</sup>,  $\Delta S^\ddagger = -29(5)$  cal·mol<sup>-1</sup>·K<sup>-1</sup>,  $\Delta G^\ddagger_{298} = 23.2(1)$  kcal·mol<sup>-1</sup>,  $R^2 = 0.993$ .

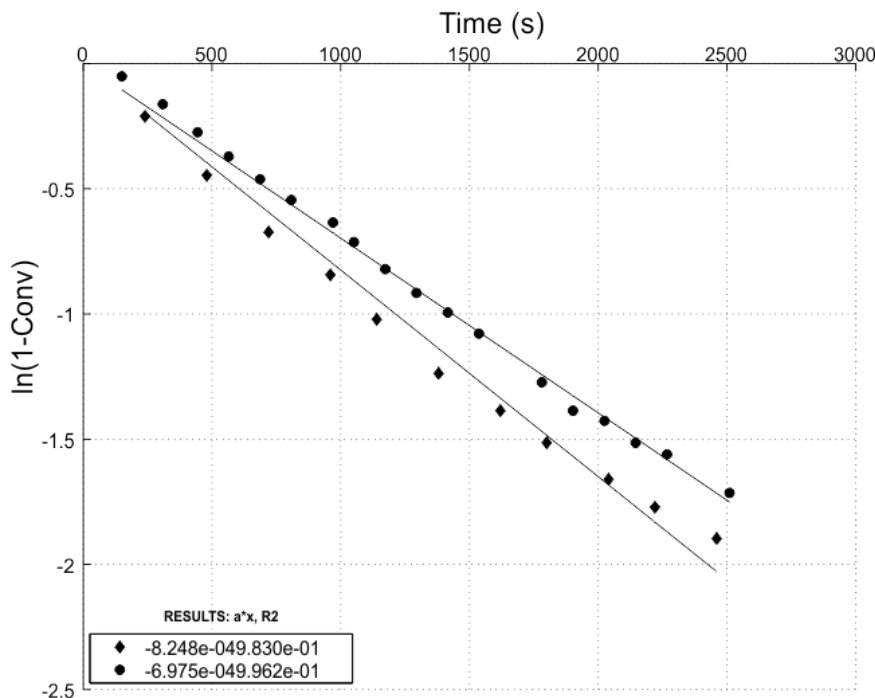


**Figure S17.** Semi-logarithmic plots for ROP of *rac*-LA at 110 °C with  $[rac\text{-LA}]_0 = 2.0 \text{ M}$  in toluene for the binary systems: ● — **I<sup>SiPh<sub>3</sub></sup>**–In,  $[rac\text{-LA}]_0/[In]/[i\text{PrOH}]_0 = 500:1:10$ ,  $k_{\text{app}} = 0.70 \pm 0.05 \cdot 10^{-3} \text{ M}^{-1}\cdot\text{s}^{-1}$ ,  $R^2 = 0.983$ ; ◆ — **II–In<sub>2</sub>**,  $[rac\text{-LA}]_0/[In]/[i\text{PrOH}]_0 = 1000:2:20$ ,  $k_{\text{app}} = 0.8 \pm 0.1 \cdot 10^{-3} \text{ M}^{-1}\cdot\text{s}^{-1}$ ,  $R^2 = 0.996$ .

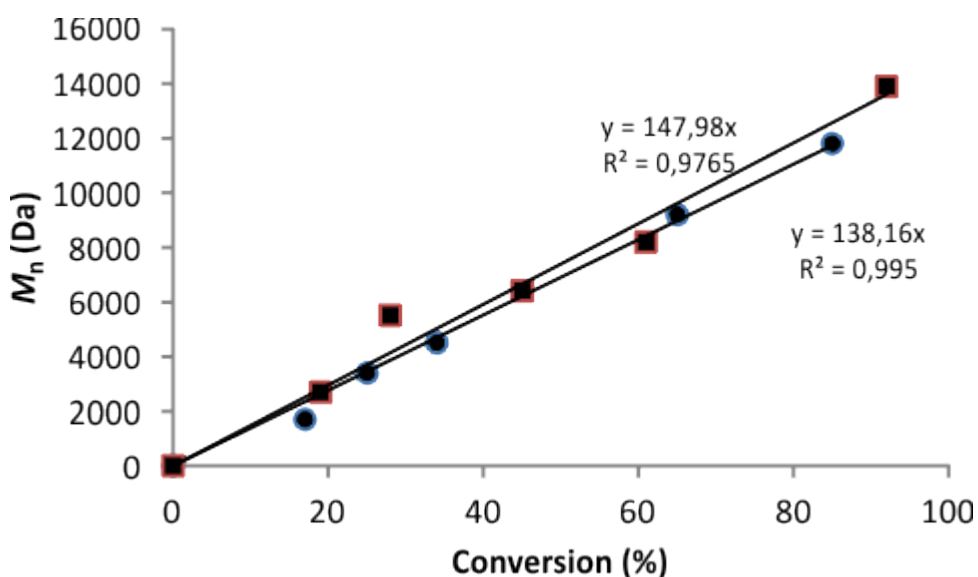


**Figure S18.** Plot of  $M_n$  vs. conversion (%) for ROP with the binary systems  $\text{I}^{\text{SiPh3}}\text{-Al}$  and  $\text{II}\text{-Al}_2/\text{iPrOH}$ ,  $[\text{rac-LA}]_0 = 2.0 \text{ M}$  in toluene at  $110^\circ\text{C}$ : ● —  $\text{I}^{\text{SiPh3}}\text{-Al}$ ,  $[\text{rac-LA}]_0/[\text{Al}]/[\text{iPrOH}]_0 = 500:1:5$ ; ■ —  $\text{II}\text{-Al}_2$ ,  $[\text{rac-LA}]_0/[\text{Al}]/[\text{iPrOH}]_0 = 1000:2:10$ .

## References and notes

- <sup>1</sup> H.-C. Zhang, W.-S. Huang, L. Pu, *J. Org. Chem.* **2001**, *66*, 481-487.
- <sup>2</sup> T. V. Hansen, L. Skattebol, *Organic Syntheses*, **2005**, *82*, 20, 64-68.
- <sup>3</sup> M. Normand, V. Dorcet, E. Kirillov, J.-F. Carpentier, *Organometallics*, **2012**, *32*, 1694–1709.
- <sup>4</sup> A. Kowalski, A. Duda, S. Penczek, *Macromolecules* **1998**, *31*, 2114-2122.
- <sup>5</sup> (a) A. Altomare, M. C. Burla, M. Camalli, G. Cascarano, C. Giacovazzo, A. Guagliardi, A. G. G. Moliterni, G. Polidori, R. Spagna, *J. Appl. Cryst.* **1999**, *32*, 115-119. (b) G. M. Sheldrick, SHELXS-97, Program for the Determination of Crystal Structures, University of Goettingen (Germany), **1997**. (c) G. M. Sheldrick, SHELXL-97, Program for the Refinement of Crystal Structures, University of Goettingen (Germany), **1997**. (d) G. M. Sheldrick, *Acta Cryst.* **2008**, *64*, 112-122.
- <sup>6</sup> L. J. Farrugia, *J. Appl. Cryst.* **1999**, *32*, 837.